3rd International Conference on New Developments in Soil Mechanics and Geotechnical Engineering,
28-30 June 2012, Near East University, Nicosia, North Cyprus

Performance of Piles in Liquefiable Soils using Numerical Analysis

Morteza Jiryaei Sharahi
Assistant Professor, Civil Engineering, Qom University of Technology, Qom-Iran
E-mail: jiryaei@yahoo.com or jiriay.m@qut.ac.ir

KEYWORDS: pile performance, earthquake, soil Liquefaction, finite difference

ABSTRACT: Liquefaction-induced lateral spreading has caused significant damage to pile foundations during past earthquakes. Ground displacements due to lateral spreading can impose large forces on the overlying structure and large bending moments in the laterally displaced piles. In order to determine the various factors affecting the behavior of piles in liquefiable soil which is underlain by non-liquefiable soil, Finite Difference Method has been used. Maximum lateral displacement and maximum pile bending moment are obtained for different thicknesses of liquefiable soil and concrete pile diameters. Results show that the failure mode of the pile significantly depends on the depth of the liquefied layer. The pile is more susceptible to buckling instability because of large values of pile lateral-displacement due to liquefaction.

1 INTRODUCTION

In liquefiable soils, progressive build up of pore water pressure may result in loss of strength and stiffness resulting in large bending moments and shear forces on the pile. Serious structural damages can be produced only when the upper part of the soils is liquefied, such as the 1964 Niigata earthquake (Hamada 1992), the 1995 Kobe earthquake (Tokimatsu 2003) and the 1999 Chi-Chi earthquake (Hwang et al. 2003), which had left extensive damage to many pile foundations of bridges and buildings.

The mechanism of pile behavior in liquefiable soil has been investigated by several investigators in the recent years; Bhattacharya et al. proposed an alternative mechanism of pile failure in liquefiable deposits during earthquakes. It was considered that the pile becomes unstable under axial load from loss of support from the surrounding liquefied soil, provided the slenderness ratio of the pile in the unsupported zone exceeds a critical value (Bhattacharya et al. 2004). The instability causes the pile to buckle and cause a plastic hinge in the pile. In terms of soil pile interaction, the method assumes that, during instability, the pile pushes the soil. Hence, the lateral load effects are considered secondary to the basic requirement that piles in liquefiable soils must be checked against Euler's buckling. However, this method can only consider one plastic hinge instead of two plastic hinges, which are observed at the interfaces of the liquefiable soil layer sandwiched between two non liquefiable soil layers. Meyerhosn proposed that piles subject to lateral spreads resulting from soil liquefaction might cause two distinct failure modes. The first one is lateral pile deflections induced by ground lateral spreads that may result in the pile reaching its

bending capacity and hence develops a plastic hinge (Meyerhosn 1994). Another failure mode is the combined action of lack of sufficient lateral support due to the reduced stiffness of the liquefied soil and the lateral deflection imposed on the pile, which may result in pile buckling. Whether bending or buckling mode of a pile may develop depends primarily on the stiffness of the liquefied soil, length of pile exposed to liquefied soil, axial load imposed to pile, and bending stiffness of the pile. However, only bending failure analysis was conduced for the evaluated case histories. Lin et al. back studied possible failure modes of three case histories. Whether these piles failed by either bending or buckling mode were re-evaluated (Lin et al. 2005). The design procedures suggested by Tokimatsu et al. (Tokimatsu et al. 1998) and by JRA (1996) were also used for case histories evaluation and compared to available observation results.
This paper examines the response of a single pile in a liquefiable soil for different depths of liquefied soil. The depth of liquefied soil not only influences the drag forces in the pile for bending calculations but also determines the length of the unsupported pile leading to lateral instability. A finite difference model, known as fast Lagrangian analysis of continua (FLAC) (Itasca Consulting Group, Inc. 2006), is used to study the pile behavior considering a nonlinear constitutive model Byrne, Finn model Byrne formulation (Byrne 1991), and pile soil interaction.

2 FINITE DIFFERENCE MODEL

The pile response is obtained using numerical analysis by the finite difference program, FLAC Itasca Consulting Group, Inc. 2006. The formulation is coupled to the structural element model, thus permitting analysis of soil structure interaction brought about by ground shaking. The analysis includes coupled mechanical and fluid flow behavior. Dynamic soil-structure interaction is captured using the hysteretic curves and energy-absorbing characteristics of the soil. The analysis is conducted using dynamic coupled mechanical / groundwater simulations with various stages. Prior to performing a dynamic simulation with ground water present, an equilibrium state is obtained. At the initial stage coupled flow and mechanical calculation is done considering fluid bulk modulus and permeability. The fluid flow is prevented since the consolidation process is not the major concern. After these analyses the system achieves mechanical and fluid equilibrium condition. The response of the pile is observed by applying an earthquake excitation. It is assumed that no fluid flow occurs due with in the short duration of excitation and hence fluid flow is prevented through the boundary. The pore pressure changes due to dynamic volume changes induced by the seismic excitation are observed.

FLAC has a simple built-in constitutive model proposed by Byrne for liquefaction analysis and their recoverable volumetric strain and pore water pressure is computed during the cyclic loading. The Byrne model considers the soil behavior due to cyclic loading such as energy dissipation and volume changes. In loose sands pore pressure may build up considerably due to cyclic shear loading. Eventually by this process effective stress approaches to zero. The constitutive model uses a few soil parameters and is related to the SPT-N value of the soil. The model is given by

$$\frac{\Delta\varepsilon_{vd}}{\gamma} = C_1 \exp\left[-C_2 \exp\left(\frac{\varepsilon_{vd}}{\gamma} \right) \right] \tag{1}$$

where $\Delta\varepsilon_{vd}$ = incremental volume strain; ε_{vd}= accumulated volume strain; γ=cyclic shear strain amplitude; and C_1 and C_2 = constants, where $C_2 = 0.4/C_1$ and C_1 can be represented with the other parameters as follows:

$$C_1 = 7600(D_r)^{-2.5},\ D_r = (N_1)_{60}^{0.5},\ \text{or}\ C_1 = 8.7(N_1)_{60}^{-1.25} \tag{2}$$

$(N_1)_{60}$= normalized SPT-N value with respect to overburden pressure of 100 kPa and corrected to a ratio of 60% and Dr = relative density. The Hardin-Drnevich model (Hardin-Drnevich 1972) is used for the representation of the variation in shear modulus and hysteretic damping with cyclic

strain. The $(N_1)_{60}$ values are obtained from corrected N values using the relationship given by Kramer (Kramer 2003)

$$(N_1)_{60} = NC_N \frac{E_m}{0.6E_{ff}} \quad (3)$$

where N=measured penetration resistance; C_N= over burden correction factor; E_m = actual hammer energy; and E_{ff}= theoretical free-fall hammer energy. E_m is considered as 0.72 E_{ff}. The value of C_N is given as

$$C_N = \sqrt{1/\sigma_{v0}} \quad (4)$$

where σ_{v0} = vertical effective overburden pressure in tons/ft^2. The other soil parameters, namely, small strain shear modulus (G_{max}), bulk modulus (K), and the friction angle (φ) are established on the basis of correlation with $(N_1)_{60}$. The soil medium is discretized into a number of four-noded quadrilateral finite difference grids. The dynamic loading is applied by a horizontal acceleration history as a boundary condition at the base. Wave reflections at model boundaries are minimized by specifying free-field boundary conditions at the two sides. Free-field boundary condition enforces the free-field motion in such away that boundaries retain their nonreflecting properties; i.e., outward waves originating from the structure are properly absorbed. The pile is modeled using linearly elastic beam elements with interface properties termed as pile element. Each element has three degrees of freedom two displacements and one rotation at each node. The analysis of piles is basically a 3D problem. In the present case, plain strain analysis is conducted. The analysis is for the response of a single pile under earthquake conditions. For the pile element elastic modulus, stiffness of the interface springs and pile perimeter are given. The element represents the response of the plate element rather than a circular section.

Bam earthquake (Mw=6.6, 2003) time history scaled with peak ground acceleration of 0.5g is considered for the dynamic analysis. Figure 1 shows scaled time history of acceleration of Bam earthquake.

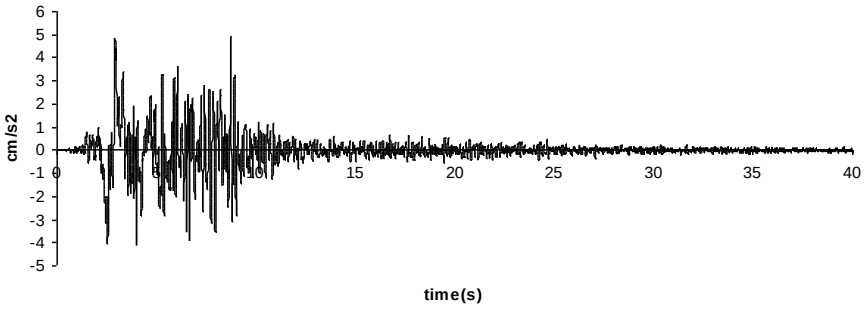

Figure 1. Acceleration time history of Bam earthquake (Mw=6.6).

The finite difference model has been validated by Haldar and Babu (Haldar & Babu 2010) using Wilson's centrifuge test data to observe soil and pile responses in liquefied sand. Wilson et al. (Wilson et al. 2000) used a two horizontal layered soil profile using saturated, fine, and uniformly graded Nevada sand prepared for the centrifuge test. The centrifuge model test has been simulated using finite difference program to validate the constitutive model used for the analysis. The numerical analysis results have been compared with the available results from the centrifuge test. Figure 2 shows the excess pore water pressure ratio time history from centrifuge test and numerical model. It is observed that the results from the finite difference model and centrifuge test results match reasonably well.

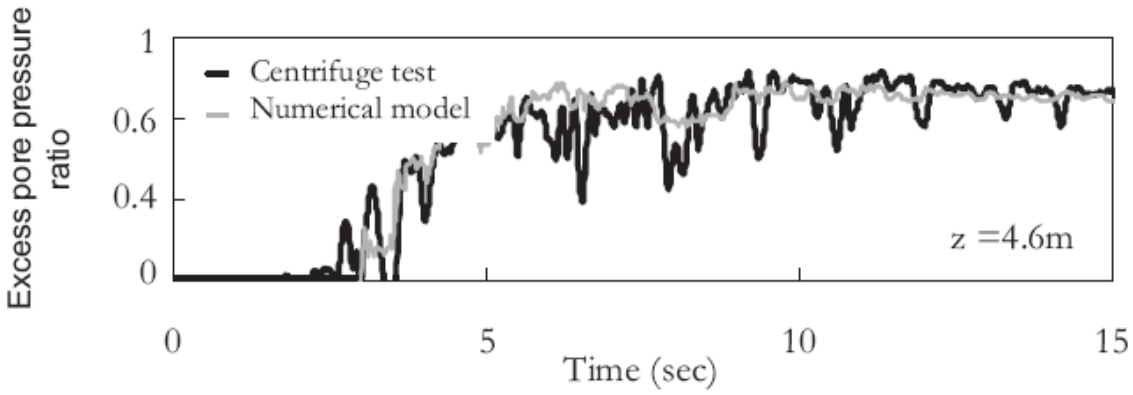

Figure 2. Comparison of excess pore water pressure ratio time history from the test and numerical model (after Haldar & Babu, 2010).

3 PARAMETRIC ANALYSIS

A schematic diagram of a numerical model is presented in Fig. 3. A parametric study is conducted considering various soil and pile parameters. Three different soil relative densities 45, 60 and 75 percent which represent loose, medium and dense sand deposits, respectively, are considered. The soil parameters used for the analysis are given in Table 1. The range of shear modulus and effective friction angle of the soil vary from 9,000 to 30,000 kPa and 26°–38°, respectively. Soil depth and lateral dimension of soil media are considered as 20m and 60 m, respectively, in the numerical model. The water table is considered to be present at the ground level. A 16 m length single pile is considered.

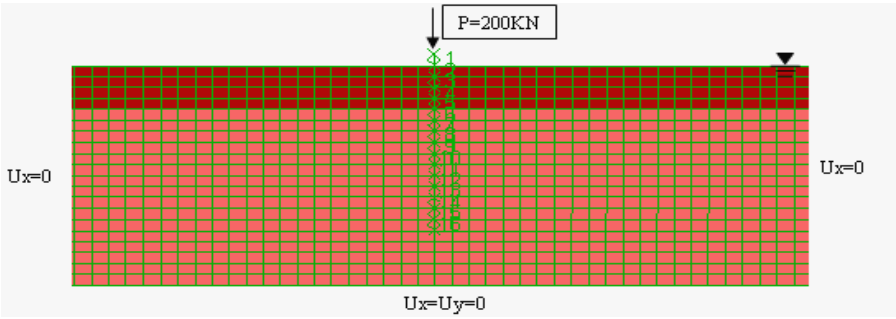

Figure 3. Numerical model of soil-pile system.

Table 1. Soil properties for the Numerical model.

Properties	*Loose Sand*	*Semi-dense*	***Dense Sand***
Dr (%)	45	60	75
Dry Density (kg/m^3)	1470	1630	1800
Porosity	0.43	0.4	0.37
Shear Modulus, G (MPa)	9	20	30
Bulk Modulus, K (MPa)	15	34	50
Friction Angle (φ)	26	32	38
Permeability (m/s)	$10^{-9} \times 8$	$10^{-9} \times 6$	$10^{-9} \times 5$
$(N_1)_{60}$	9	16	25

Table 2. Pile properties for the Numerical model.

Properties	D_P = 0.6 m	D_P = 0.8 m
Pile length below ground (m)	15	15
Pile length above ground (m)	1	1
Density (kg/m^3)	2500	2500
Flexural strength, fy (Kpa)	$10^4 \times 1.12$	$10^4 \times 1.12$
Yeild moment of pile, My (Kn.m)	237	560
Modulus of elasticity, Ep (Kpa)	$10^4 \times 3$	$10^4 \times 3$
Moment of inertia, Ip (m^4)	0.006	0.02
Pile Perimeter (m)	1.885	2.513
Cross – Sectional area, Ap (m^2)	0.283	0.502

The pile is embedded in the ground by 15 m and 1m above the soil surface. Three different liquefiable soil thicknesses of 4 m, 6 m, and 8 m, and different concrete-pile diameters of 0.6 and 0.8 m, are adopted for analysis. The embedded length of pile and the soil depth are considered the same to simulate an end bearing pile. The pile is discretized into 16 equal segments. The different pile parameters are given in Table 4. A rotational restraint is applied at the pile head so that it can not rotate but can laterally deflect. It is assumed that when the liquefaction starts the resistance offered at the pile head minimizes due to severe displacement, and hence the pile acts as a fixed free cantilever. Hence, at the on set of liquefaction, a free head boundary condition is imposed.

3 RESULTS AND DISCUSSION

The influences of different soil liquefiable thicknesses, soil relative densities, and pile diameters on the pile response which described in terms of maximum bending moment and maximum displacement are examined.

When a liquefiable soil layer is subjected to an earthquake loading, the pore pressure increases and that leads to soil liquefaction because the effective stress decreases toward zero. Excess pore water pressure ratios (EPWPR= u/σ) at different times of excitation at different depths of soil are obtained. Figure 4 shows obtained EPWPR and depth of liquefied layer. The soil is said to be completely liquefied when EPWPR reaches 1.0. The depth of liquefied soil layer (LL) is obtained where EPWPR is greater than or equal to 1.0 over the entire soil layer. Soil with relative densities of 60 and 75 % have EPWPR less than 1.0, hence liquefaction may not occur.

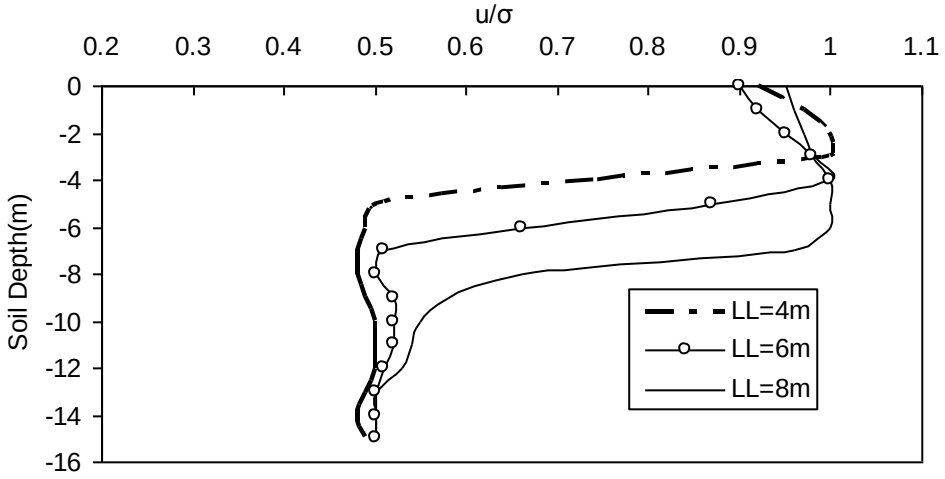

Figure 4. EPWPR for liquefied soil depths of 4 m, 6 m and 8 m (Dr=45 %).

The bending moment developed in the pile section is observed over the pile length and the value of maximum bending moment over the pile length is considered at different times of excitation. It can be stated that the pile is said to have failed due to bending if the maximum bending moment (M_{max}) value in the pile exceeds the yield moment (M_y) value of the pile section. Figure 5 shows M_{max}/M_y for different liquefied depths and pile diameters. Bending failure of pile occurs when the ratio of developed maximum bending moment value and yield moment value of the pile section, i.e., M_{max}/M_y value exceeds 1.0 such as liquefied layer depths of 6m and 8m from figure 5.

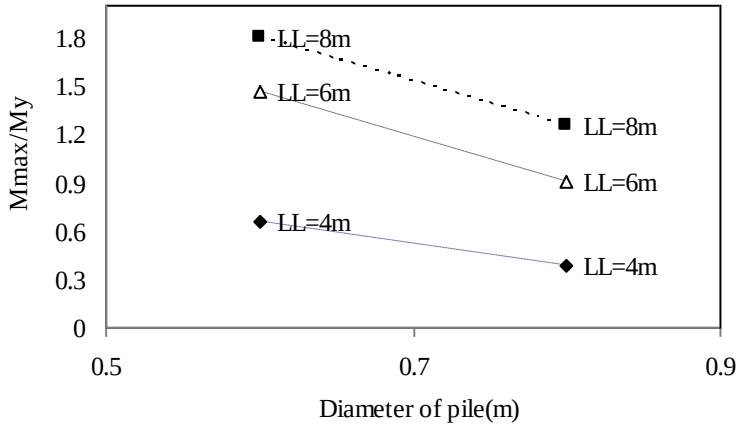

Figure 5. M_{max}/ M_y ratio for different liquefied depths and pile diameters.

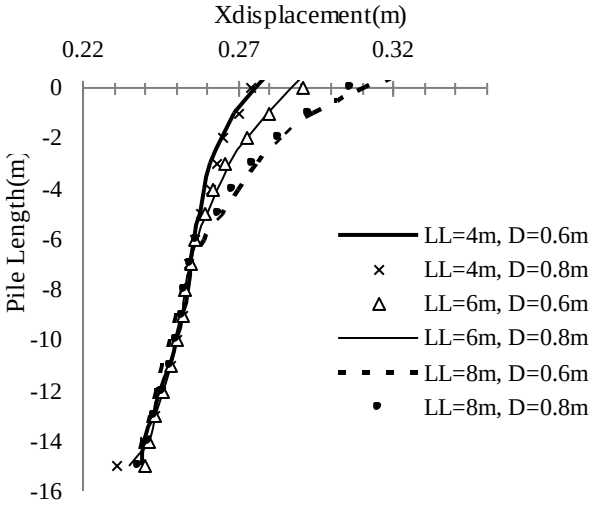

Figure 6. Maximum lateral pile displacement obtained from the numerical model.

It should be noted that other failure mechanism is the pile buckling. It is observed that the pile starts to deflect abruptly when critical buckling load is almost three times the applied load. Hence, the pile is considered to be susceptible to buckle when the P/P_{cr} value exceeds 0.33. Figure 6 shows a large value of Pile lateral displacement due to earthquake excitation. Hence it can be stated that the pile is more susceptible to buckling instability.

4 CONCLUSION

The effects of soil relative density, liquefiable soil thickness, and pile diameter on the pile response in liquefiable soil are examined. The failure mode of the pile significantly depends on the depth of the liquefied layer. Bending failure of pile occurs if maximum bending moment value in the pile exceeds the yield moment value of the pile section. The pile is more susceptible to buckling instability because of large values of Pile lateral-displacement due to liquefaction during earthquake.

REFERENCES

Abdoun, T. and Dobry, R. (2002). Evaluation of pile foundation response to lateral spreading. *Soil Dyn. Earthquake Eng.*, 22, 1051–1058.

Abdoun, T., Dobry, R., O' Rouke, T. D., and Goh, S. H. (2003). Pile response to lateral spreads: Centrifuge modelling. *J. Geotech. Geoenviron. Eng*., 129(10), 869–878.

Bhattacharya, S., Madabhushi, S.P.G., and Bolton, M.D. (2004). An alternative mechanism of pile failure in liquefiable deposits during earthquakes. *Geotechnique*, 54(3), 203-213.

Byrne,P. (1991). A cyclic shear-volume coupling and pore pressure model for sand. *Proc. Of 2nd International Conf. on Recent Advances in Geotechnical Earthquake Engineering and Soil Dynamics*, St.Louis, 47–55.

Finn, W. D. L., and Fujita, N. (2002). Piles in liquefiable soils: Seismic analysis and design issues. *Soil Dyn. Earthquake Eng*., 22, 731–742.

Haldar, S. and Babu, G.L. (2010). Failure Mechanisms of Pile Foundations in Liquefiable Soil: ParametricStudy, *International Journal of Geomechanics*, 10(2), 74-84.

Hamada M. (1992). Large Ground Deformations and Their Effects on Lifelines: 1964 Niigata Earthquake in Case Studies of Liquefaction and Lifeline Performance During Past Earthquakes. Japanese Case Studies, Technical Report, NCEER-92-0001, NCEER, Buffalo, NY, USA, Vol. (1), 3.1-3.123.

Hardin, B. O. and Drnevich, V.P. (1972) . Shear modulus and damping in soils: Design equations and curves. *J. Soil Mech. And Found*. Div. 98(7), 667–692.

Hwang, J.H., Yang, C.W., Chen, C.H. (2003). Investigations on soil liquefaction during the Chi-Chi earthquake. *Soils and Foundations*, 43(6), 107-123.

Itasca Consulting Group, Inc. (2006). Fast Lagrangian analysis of continua (FLAC); user's manual, 2006.

Japanese Road Association (JRA), (1996). Specification for high way bridges, part. V: Seismic design. JRA, Tokyo.

Kramer, S. L. (2003). *Geotechnical earthquake engineering*, Pearson Education , NewDelhi.

Lin, S. S., Tseng, Y. J., Chiang, C. C., and Hung, C. L. (2005). Damage of Piles Caused by Lateral Spreading- Back Study of Three Cases in Seismic Performance and Simulation of Pile Foundations in Liquefied and Laterally Spreading Ground, *GSP* No. 145, *ASCE*, 121-133.

Meyersohn, W. D. (1994). Pile response to liquefaction-induced lateral spread. *Doctor's dissertation*., Cornell University, USA.

Tokimatsu, K., Oh-oka, H., Satake, K., Shamoto, Y., and Asaka, Y. (1998). Effects of Lateral Ground Movements on Failure Patherns of Piles in the 1995 Hygoken-Nambu Earthquake. *Geotechnical Earthquake Engineering and Soil Dynamics*, Vol. (3), 1175-1186.

Tokimatsu, K. (2003). Behavior and design of pile foundations subjected to earthquakes. *Keynote Speech, 12th Asia Regional Conference on Soil Mechanics and Geotechnical Engineering*, Singapore, Vol. (2), 1065-1096.

Wilson, D.W., Boulanger, R.W., and Kutter,B.L. (2000). Observed seismic lateral resistance of liquefiable sand. *J. Geotech. Geoenviron. Eng*., 126(10), 898–906.